Fabrication of Cube Beamsplitters for White Light Interferometry

Peter D. Koudelka[a], James H. Burge[b]

[a]PROMET International Inc., 4611 Chatsworth St., Shoreview, MN USA 55126;
[b]Optical Sciences Center, University of Arizona,
1630 E University Blvd., Tucson, AZ USA 85721

ABSTRACT

Interferometric applications utilizing short coherence length sources, such as white light interferometry, require precise matching of optical path lengths for the two arms of the interferometer. If a cube beamsplitter element is utilized, the added dispersive material in the optical path could introduce undesirable optical path difference (OPD) effects and a consequent degradation in fringe visibility. For this reason a cube beamsplitter must be well matched for equal geometric path length in glass during the fabrication process. Two degrees of freedom must be controlled; the lateral position and relative rotation of the two prisms that comprise the beamsplitter. A method is described for efficiently assembling cubed beamsplitters utilizing a kinematic mount to adjust the relative position of the beamsplitter prisms with sub-micron precision for both degrees of freedom. The OPD is monitored simultaneously at three separate wavelengths during assembly by exploiting the color separation capabilities of a spatially congruent 3-CCD color camera. Once positioned to minimize the OPD, the prisms are bonded together with UV curing adhesive and any residual aberrations are quantified. The technique was proven by aligning prisms to 0.1μm accuracy and measuring the OPD error to 0.05μm accuracy.

Keywords: White light interferometry, cube beamsplitters, beamsplitter fabrication

1. INTRODUCTION

White light interferometry offers a distinct advantage over monochromatic interferometry by eliminating the 2π modulo ambiguity associated with interference periodicity of single laser source systems. This advantage is based on the principle that acceptable fringe visibility only occurs when both arms of the interferometer have matching optical path lengths (OPL) for each wavelength of the broadband light source.

This characteristic allows white light interferometry concepts to be used in various applications where an absolute determination of the optical path length is required. For example, in metrology, white light interferometry allows for making accurate optical surface measurements (nanometer level) over a relatively long range (millimeters).[1-3] Numerous characterization methods of dispersion in optical fibers and other optical components also utilize white light interferometry concepts.[6, 7] Nulling stellar interferometry, proposed for the detection of extrasolar planets, relies on the precise matching of optical path lengths to cancel out bright objects located near the observation target.[8]

All of these applications require a very close control of the broadband optical path length properties of the interferometer arms for optimum performance. Since the OPL in dispersive medium varies with wavelength, cube beamsplitters used in such systems must have internally matched reflection and transmission optical path lengths to avoid introducing wavelength dependent phase errors into the wavefront.

Typical commercial cube beamsplitters are not currently manufactured to the tolerances required by white light interferometry. High quality beamsplitters are typically matched to about 100μm of optical path length and can vary significantly from one piece to the next. White light interferometers typically require a much closer control of the OPL, ranging from 0.1μm-10μm depending on the application. Some commercial cube beamsplitters optimized for equal OPL are available, however, achieving 0.1μm accuracy is often prohibitively expensive and difficult to accomplish, making their use for production applications impractical.[1] This leads to the need of developing an efficient method for the fabrication and testing of cube beamsplitters with sub-micron OPL variations.

A previously proposed testing method utilizing a tunable dye-laser to optically quantify the OPL of beamsplitter arms works well for quantifying large OPL variations on the order of several microns.[5] However, the accuracy of this method has been proven to only about 1μm, which may not be sufficient for some applications. This method also relies on specialized equipment that may not be readily available for fabrication purposes.

We present a practical solution for the fabrication of cube beamsplitters through the use of an integrated optomechanical system to quickly and easily achieve a high accuracy of optical path matching in a low-volume production environment. Building on the concepts of the tunable dye-laser measurement technique, we propose a more efficient method using a standard white light source and a commercially available 3-CCD color camera. This method allows for a quicker and more accurate determination of OPL properties, is insensitive to prism coatings, and has the added benefit of quantifying residual OPL variations. Quality requirements for prism substrates are addressed and related to the overall optical characteristics of the assembled beamsplitter. Finally, we present data showing that beamsplitters were successfully matched to less than $0.1\,\mu m$ of on-axis optical path length variations.

2. REQUIREMENTS FOR WHITE LIGHT INTERFEROMETRY

White light can be thought of as a superposition of an infinite number of coherent waves over a finite and continuous spectral range. In a white light interferometer these monochromatic carriers generate a discrete set of periodic fringes with spatial frequencies corresponding to their wavelengths. When the intensity values of these fringe patterns are summed, then acceptable fringe visibility is limited to a single finite coherence packet. The length of this coherence packet is referred to as the coherence length (ℓ_c) and is approximated by the expression

$$\ell_c = \frac{\lambda_o^{\,2}}{\Delta\lambda}\,, \tag{1}$$

where $\Delta\lambda$ is the FWHM value of the spectral distribution and λ_o is the center wavelength.[9] The coherence packet is centered on a single fringe that indicates a unique location where the optical path lengths of both interferometer arms are perfectly matched. This point is referred to as the center fringe.

The optical path length of a wavefront passing through a dispersive material is defined by the expression

$$OPL(\lambda,t) = \int n_\lambda(t)dt\,, \tag{2}$$

where n_λ is the index of refraction at wavelength λ and t is the thickness of dispersive material. An interferometer splits light into two beams that are then recombined to produce interference. As the two separate beams propagate, the total distance traveled by one beam will be different from the other. We define this as the optical path difference (OPD) error. When two such beams interfere, the maximum fringe contrast will occur when the optical path difference between the beams is minimized for each wavelength component. Therefore, to achieve maximum fringe contrast a white light based interferometer requires that the OPD between the two interferometer arms is zero, or equivalently when

$$OPD = \Delta OPL(\lambda,t) = 0\,. \tag{3}$$

In order to satisfy the requirement in Eq. 3 the optical path lengths AC and AE shown in Figure 1 must be equivalent for optimal fringe contrast.
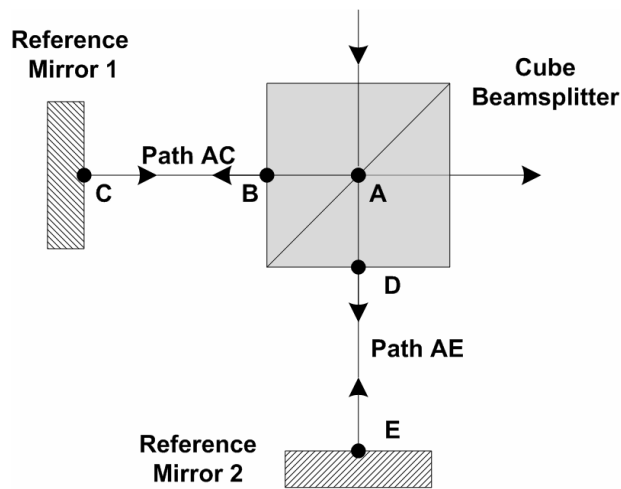

Fig 1. The optical path length AC and AE of a white light based interferometer must be matched to preserve coherence.

It is always possible to match the OPL for any single wavelength by translating one of the reference mirrors, or equivalently by changing the length of distance BC. However, when multiple wavelengths are present, the system can only be achromatized by matching the amount of glass in each arm. This means that lengths AB and AD as well as BC and DE must be equivalent. This is due to the inherent dispersive nature of optical glass. It is worth pointing out that for some applications acceptable fringe contrast will still be achieved if the difference between optical path ACA and AEA is less than the length of the coherence packet ℓ_c. If the OPD error is greater than ℓ_c, then fringes are not visible.

3. OPD ERRORS IN CUBE BEAMSPLITTERS

A well-matched cube beamsplitter is composed of two high quality prism substrates precisely bonded together at the hypotenuse to form an optically symmetrical cube element. The final quality of the beamsplitter is dependent on the fabrication accuracy of the substrates as well as the relative alignment accuracy of the prism elements during bonding. Both kinds of errors must be considered in evaluating the overall beamsplitter performance. An incorrectly fabricated cube beamsplitter can introduce significant OPD effects into a system as the two optical arms travel through uneven amounts of glass (ΔS). In the case of white light interferometry, these effects lead to wavelength dependent phase errors and contribute to fringe contrast deterioration during wavefront recombination and interference. This section addresses some of the main sources of OPD errors in cube beamsplitters and how these errors relate to the physical fabrication tolerances of the optical elements.

3.1 Substrate Errors

Substrate manufacturing uncertainties, which are inherent to every manufacturing process, are deviations from the nominal values of the prism element physical properties. Specifications of allowable tolerances should be determined by the performance requirements of the system and the expenditure of time and money that is justifiable for the application.[10] In volume production situations, it becomes highly desirable to quantitatively define the relationship between tolerance values and final performance of an assembled beamsplitter cube in order to minimize the cost of fabrication.

The key prism substrate properties that affect the OPD performance of a beamsplitter are:
- Geometrical properties – Angular deviation
- Surface properties – Surface form deviation
- Material properties – Glass homogeneity

It is convenient to think of these substrate fabrication errors as thin pieces of glass of thickness ΔS placed in front of a perfect element (See Fig 2). The thickness ΔS corresponds to the maximum deviation from the ideal shape or property of the substrate and can be derived for each beamsplitter geometry. The collective effect of the prism substrate fabrication errors on a plane wave passing through the beamsplitter can be modeled as a series of these thin elements placed in the optical path of both the transmitted and reflected beams of an ideally perfect beamsplitter.
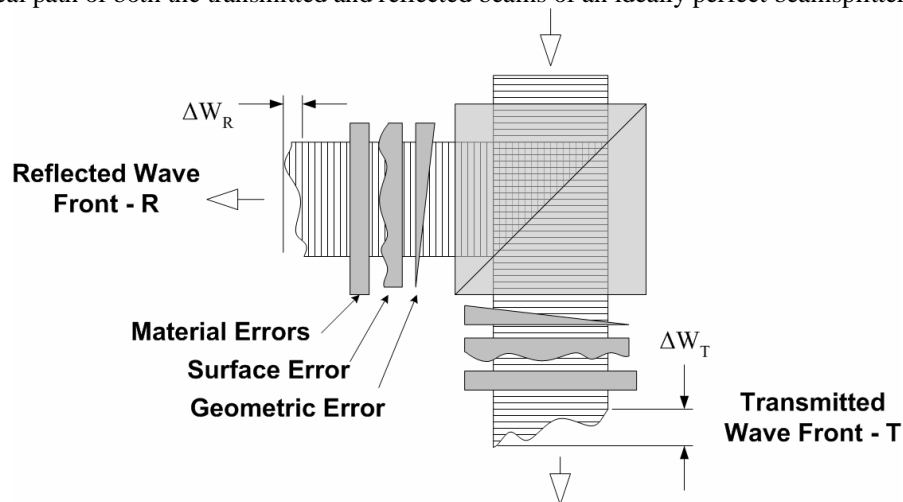

Fig 2. Substrate fabrication errors represented as thin pieces of glass placed in each arm of an ideally perfect beamsplitter.

The maximum wavefront deviation (ΔW) for each beamsplitter arm can be estimated by summing the OPL effects induced by the substrate fabrication errors

$$\Delta W(\lambda) = \sum_{Errors} \Delta S \cdot (n_\lambda - 1), \tag{4}$$

where n_λ is the index of refraction at the center wavelength λ. The difference between the wavefront deviations of the two arms is the OPD error in the beamsplitter contributed by the fabrication errors of the prism substrates. This can be defined as

$$OPD_{FAB}(\lambda) = \Delta W_R - \Delta W_T, \tag{5}$$

where ΔW_R and ΔW_T represent the maximum wavefront distortion values for the reflected and transmitted arms respectively.

3.2 Assembly Errors

A second factor contributing to the OPD error of a cube beamsplitter is the alignment of the two prism substrates during beamsplitter assembly. The alignment process is often the limiting factor in minimizing the total internal OPD errors and represents the most challenging step in beamsplitter fabrication.

There are two critical degrees of freedom (DOF) that need to be controlled during the assembly process as shown in Figure 3. They are the lateral translation along the X-axis of the prisms in the hypotenuse plane (DOF_1), and the rotation of the prisms about an axis perpendicular to the hypotenuse plane (DOF_2). Each of these degrees of freedom will contribute to the overall OPD error of the beamsplitter.

The relative lateral position of the prisms along the X-axis (DOF_1) is the most critical adjustment. This degree of freedom is essentially used to match the on-axis optical path length of the two arms within the beamsplitter and is usually the largest source of OPD error. The second degree of freedom (DOF_2) is used to effectively eliminate any pyramid error that might be present in the prisms by ensuring that both the exit faces of the beamsplitter cube are perpendicular to the incoming optical axis.

Utilizing a concept similar to the modeling of prism substrate errors, alignment errors can also be represented as thin optical elements placed in the path of an ideally perfect beamsplitter as shown in Figure 4. The relative linear misalignment (DOF_1) of the prisms can be modeled as a parallel plate of glass with a varying thickness (ΔS). Similarly, the relative rotational misalignment of the prisms (DOF_2) can be modeled as a wedge of glass with a varying angle and a maximum thickness of (ΔS). Both values of ΔS can be derived from the specific geometry and size of the beamsplitter.
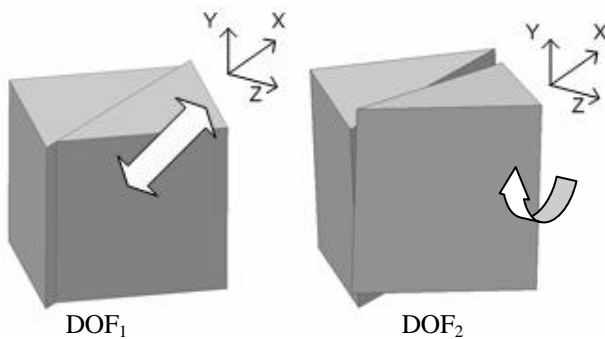

Fig 3. Two critical degrees of freedom exist when assembling the two prism substrates that form a cube beamsplitter. They are DOF_1 and DOF_2.
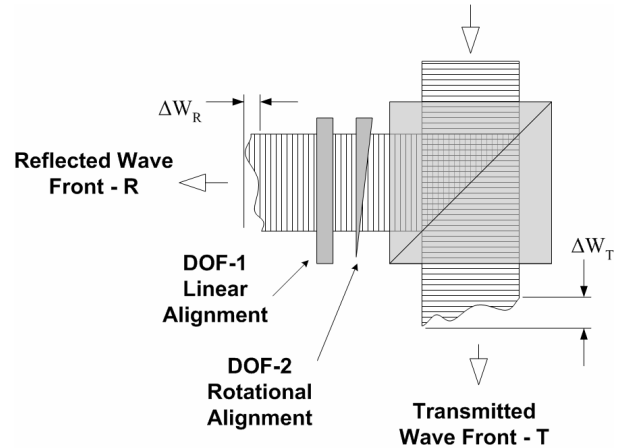

Fig 4. Alignment errors of the beamsplitter can be modeled as additional, thin pieces of glass placed in the optical path of an ideal beamsplitter cube.

The UV adhesive layer between the two prisms will be several microns thick (depending on adhesive viscosity) and will have the effect of introducing a separation between the two prisms. This gap thickness can be compensated for by the linear prism motion along the X-axis (DOF_1). For this reason, the thickness of the glue gap is not a factor in overall alignment accuracy.

The maximum OPD error in the beamsplitter due to alignment errors is the summation of the OPL effects of the two thin glass elements. Therefore, the alignment OPD error in terms of additional glass in one arm is expressed as

$$OPD_{AL}(\lambda) = \sum_{Errors} \Delta S \cdot (n_\lambda - 1).$$ (6)

3.3 Summary of Error Contributions

The total OPD performance of the beamsplitter is the summation of the errors contributed by the prism substrates and errors contributed by the alignment of the prism substrates. The total OPD error present in an assembled beamsplitter over the full aperture is expressed as

$$OPD_{TOTAL}(\lambda) = OPD_{FAB}(\lambda) + OPD_{AL}(\lambda).$$ (7)

The equivalent phase variation over the aperture is determined by the expression

$$\Delta\phi(\lambda_o)_{TOTAL} = \frac{2\pi}{\lambda_o}\left(OPD(\lambda_o)_{TOTAL}\right),$$ (8)

where λ_o is the center wavelength of the light source being used. It is important to note that the values for the individual OPD contributors must be calculated for a corresponding value of λ. The value of OPD_{TOTAL} can simply be doubled to find the total OPD error introduced by a beamsplitter used in a double-pass configuration as is the case with most white light interferometers.

4. OPD MEASUREMENT

OPD within the beamsplitter is determined by utilizing the limited coherence of white light and the chromatic separation capabilities of a 3-CCD RGB camera. A 3-CCD camera uses a dichroic micro-prism assembly to chromatically separate incoming light into three separate bands centered at 645nm(R), 545nm(G), and 460nm(B). Each channel is imaged onto a separate monochromatic CCD area detector resulting in co-spatial intensity information at three separate wavelengths.

The simultaneous monitoring of the R, G, and B spectral bands facilitates easy identification of the zero-OPD fringe without searching for the brightest fringe of the coherence packet. Figure 5 illustrates a simulated fringe intensity profile of each spectral band as seen by the three channels of the RGB camera. The black lines indicate the local apex of each fringe in the FOV for the three chromatic bands of the camera. The center zero-OPD fringe, identified by the arrow, occurs where the fringe centers correspond for all three color bands. This condition occurs exactly once within the coherence packet of the light source. A LabVIEW® program is used to identify the zero-OPD fringe and indicate its location in the FOV.
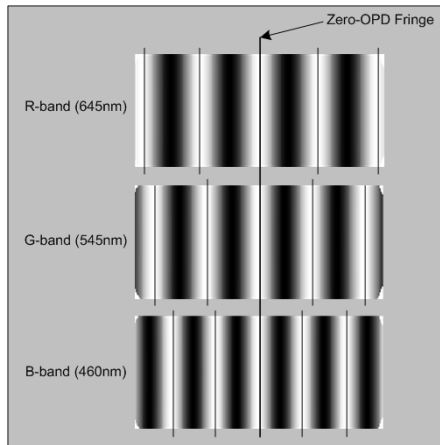

Fig 5. A simulated fringe pattern with equivalent tilt at the R, G, and B spectral bands. Arrow indicates the location of the center zero-OPD fringe.

5. EXPERIMENTAL LAYOUT

An efficient and accurate alignment of beamsplitter prism substrates is achieved through the use of an integrated optical system capable of actively monitoring the OPD properties of a cube beamsplitter during the alignment process. For this system a white light interferometer setup is used to generate white light fringes through the beamsplitter being assembled. The fringes are imaged onto three separate CCD planes of an RGB camera that samples the incoming light at three separate visible bandwidths. The signal from the camera is sent via a multi-channel frame grabber into a computer where it is processed using custom LabVIEW® code. Real-time results are displayed on a monitor allowing the user to make appropriate adjustments. Figure 6 illustrates the schematic of the system and its major components. Following sections summarize the major optical and mechanical subsystems.
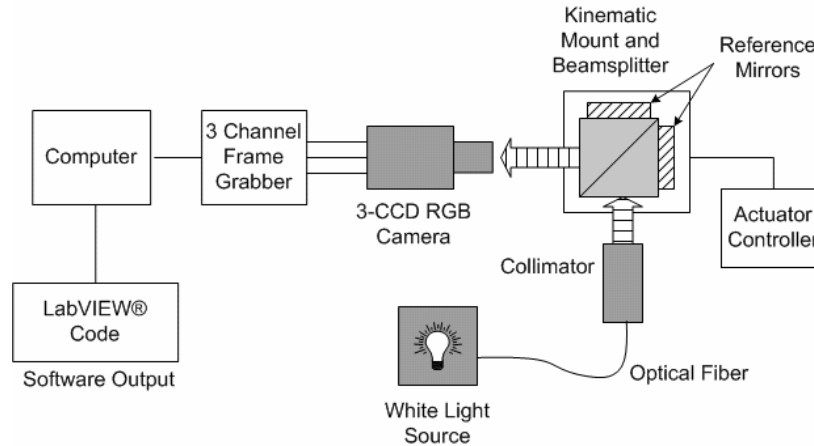

Fig 6. Schematic layout of the beamsplitter alignment and testing system. White light source is used to generate interference fringes, which are imaged onto a 3-CCD camera. A computer algorithm is used to determine the location of the zero-OPD fringe.

5.1 Optical Layout

The optical layout of the beamsplitter testing and alignment instrument is a variation on a basic Twyman-Green interferometer arrangement as shown in Figure 7. A collimated white light beam is split into a test and reference beam and then recombined to yield an interference pattern. The limited coherence of the white light source allows for the quantification of optical path length in addition to the relative wavefront distortion, as is the case in classical multi-wavefront interferometry. By utilizing two high quality reference surfaces (instead of a reference and a test surface) the beamsplitter effectively becomes the system variable that is adjusted and measured.
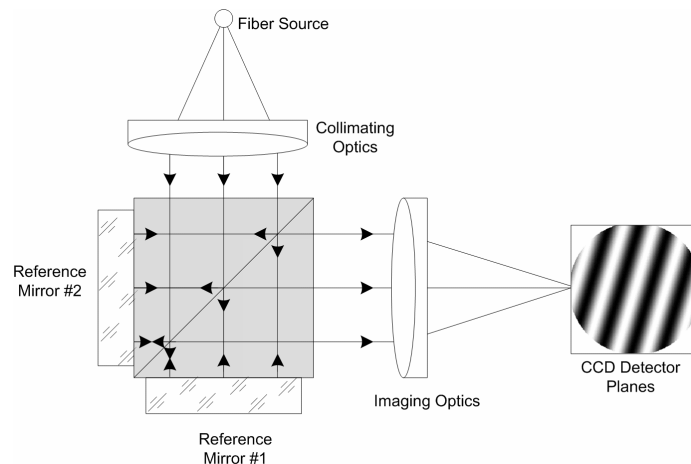

Fig 7. Optical testing scheme is a variation on a basic Twyman-Green configuration with both reference mirrors resting against the beamsplitter cube. Both mirrors act as reference surfaces and the beamsplitter is the test element.

Note that the reference mirrors do not serve the function of a retro reflector as would be the case in an ideal Twyman-Green interferometer configuration. Instead, the reference mirrors are pressed up against the exit surfaces of the beamsplitter and adapt to any angular errors that may be present in those surfaces. The tip and tilt of the mirrors are indicated by the resulting fringe pattern, which in turn provides information regarding the wedge and pyramid errors present in the beamsplitter. Good contact between the mirrors and the beamsplitters is critical to avoid introducing errors into the alignment. The contact between a coated surface and the mirror was experimentally determined to be repeatable to within about 0.5 wave of tilt.

5.2 Mechanical Layout

The alignment of the beamsplitter prism substrates is achieved by a high precision optomechanical system capable of active, sub-micron positioning over two discreet degrees of freedom. The heart of this system is a fully kinematic stage, which is used to set and maintain the precise position of the beamsplitter assembly during the fabrication process (See Figure 8).

The assembly procedure for the beamsplitter is simple, requiring only basic operator skills. First both prism substrates are cleaned and joined with a thin layer of uncured UV adhesive. The preassembled beamsplitter is then placed in the kinematic mount with both reference mirrors resting up against the exit faces of the cube. The relative position of the two prism substrates is then adjusted using two integrated actuators. First a rough alignment is done utilizing a pinhole aperture and then both DOF_1 and ODF_2 are fine tuned to the desired tolerance. DOF_1 is controlled by a New Focus™ PicoMotor™ with a linear resolution of less than 100nm, and DOF_2 is controlled by a piezoelectric actuator with a rotational resolution of less than 1 arc second. Once the beamsplitter is aligned, the UV adhesive is cured and the completed beamsplitter can be removed.
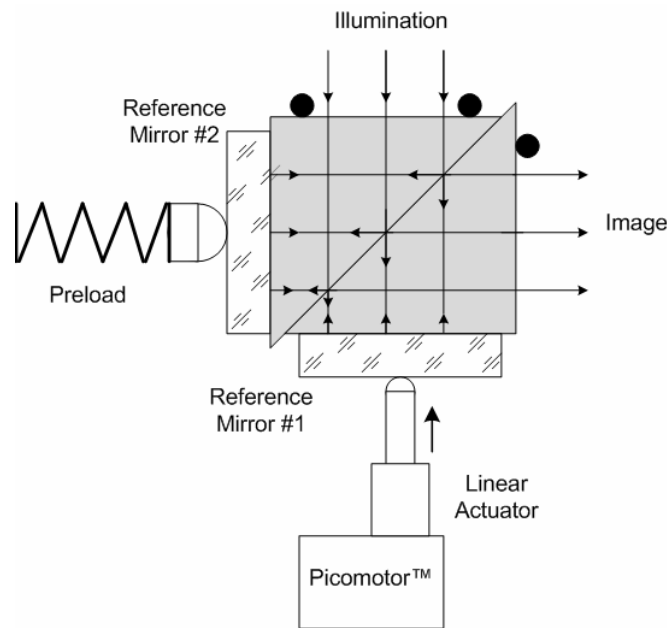

Fig 8. Kinematic stage used to align prism substrates uses two high precision actuators to independently control the two critical DOF. Piezoelectric actuator is located underneath the beamsplitter cube and is not shown.

A driving functional requirement of the stage is the mounting of the two beamsplitter prism elements in such a manner that allows for the adjustment of the two corrective DOF of the prism pair, while maintaining a consistent contact between the hypotenuse faces. In addition, the mounting scheme needs to be insensitive to minor variations in the shape of each prism due to fabrication tolerances. This requirement is satisfied by defining discreet points of contact to kinematically control all six degrees of freedom of each prism element.

Two separate actuators are used to make adjustments to the relative position of the two prisms and the two degrees of freedom that need to be controlled during the fabrication of the beamsplitter (DOF_1, DOF_2). The mount is designed so that each actuator controls exactly one degree of freedom to minimize "cross-talk" during the alignment process.

6. TEST DATA AND RESULTS

For the initial trial of the alignment system, four beamsplitters were aligned for minimum OPD error. Figure 9 contains a sample of the measurement data produced for an aligned beamsplitter. All three channels are included, representing the three color bands R, G, and B. The center fringe is the zero-OPD fringe indicating that the beamsplitter is aligned for zero-OPD on the optical axis. The vertical orientation of the fringes indicates that most of the pyramid error has been corrected out and only residual wedge error remains. The wedge error cannot be corrected during alignment and is dependent on the quality of the prism substrates.
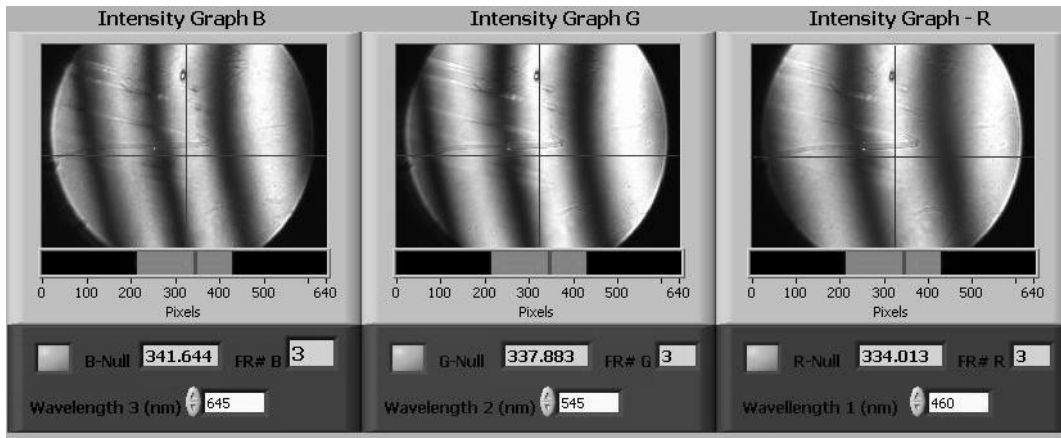

Fig 9. Sample reading for an aligned beamsplitters showing the intensity values for all three color bands (RGB). Center fringe is the zero-OPD fringe and only residual wedge error is present.

All four beamsplitters were successfully aligned for nearly zero on-axis OPD. Some residual wedge error remains causing some OPD variations over the 6mm aperture of the beamsplitter. Table 1 contains a summary of the quantitative data measured for each beamsplitter.

Beamsplitter	On-Axis OPD (µm)	OPD Variation (µm)
A	0.02	0.27
B	0.11	0.43
C	0.04	0.32
D	0.02	0.12
Average	0.048	0.285

Table 1. Summary of measured OPD errors in aligned beamsplitters for a single pass configuration.

The results of the four test beamsplitters appear to be very promising. On-axis OPD errors are less than ¼ wave for all trials. The residual OPD errors over the aperture of the beamsplitter are also very small, all staying under 1.0 wave. These beamsplitters satisfy the criteria for most white light interferometric applications with coherence lengths of more than a few waves.

7. CONCLUSION

White light interferometry and other dispersion sensitive applications require close control of the optical path length within the system. When using a cube beamsplitter in these applications a special fabrication technique is required to ensure that the beamsplitter does not introduce any OPD errors between the transmitted and reflected beams. We have shown an efficient method of fabricating cube beamsplitters matched to an accuracy of less than 0.1µm of on-axis OPD. The method presented utilizes an integrated three-wavelength OPL detection scheme and a high precision kinematic mounting approach to manipulating the prism substrates of the cube beamsplitter. In addition to determining the OPD performance of the beamsplitter, any residual OPD errors over the aperture of the beamsplitter can also be quantified.

Experimentation has shown that cleanliness of the contact between the reference mirrors and the beamsplitter is critical for proper performance of the system. Beamsplitters should be assembled in a controlled and clean environment to minimize any chances of contamination.

Further improvements in alignment accuracy are possible. The control of DOF_1 is limited by the linear resolution of the PicoMotor™ and could be improved to less than 30nm. Residual wedge error in the beamsplitter can also be reduced by improving the accuracy of the prism substrates.

Although higher accuracy is feasible, the method presented in this thesis exceeds the requirements established for most white light interferometry applications. Furthermore, the alignment is achieved with fairly low-cost instrumentation in a relatively short amount of time, making it ideal for production environments. For these reasons, the method we propose is a complete solution for the efficient fabrication of cube beamsplitters for white light interferometry applications.

REFERENCES

1. Pförner, J. Schwider, "3-λ Metrology," in *Interferometry XI: Techniques and Analysis*, K. Creath, J. Schmidt, Eds., *Proceedings SPIE* **4777**, (2002).
2. M. Krieg, R. Klaver, J. Braat, "Absolute optical path difference measurement with angstrom accuracy over ranges of millimeters," in *Optical Measurement Systems for Industrial Inspection II: Application in Industrial Design*, Proc. W. Osten, W. Juptner, M. Kujawinska, eds., *Proc. SPIE* **4398**, (2001).
3. M. Shaalan, V. Little, "The application of multiple-beam, white-light fringes to the study of surfaces," *Applied Physics* **8**, pp. 1003-1007 (1975).
4. H. McIntire, M. Fetrow, L. McMackin "Spatio-spectral phase unwrapping for multi-wavelength heterodyne interferometry," *Proc. SPIE* **3815**, (1999).
5. K. Farr, N. George, "Beamsplitter cube for white light interferometry," *Optical Engineering* **31**, pp. 2191-2196, (1992).
6. P. Hlubina, "Applications of low-coherence interferometry in fiber optics," in *Lightmetry: Metrology, Spectroscopy, and Testing Techniques Using Light*, M. Pluta, eds., *Proceedings SPIE* **4517**, (2001).
7. P. Sandoz, J. Calatroni, G. Tribillon, "White Light Interferometry: Innovative algorithms and performances," *Proc. SPIE* **3572**, (1999).
8. Rhonda Morgan, *Achromatic Nulling Beam Combiner for the Detection of Extrasolar Planet.*, PhD thesis, University of Arizona, Tucson, 2002.
9. J. Wyant, *Coherence*, OPTI505 class notes, University of Arizona, Tucson, 2002.
10. W. Smith, *Modern Optical Engineering*, McGraw-Hill, New York, 2000.